Optimization of High-Order Harmonic Generation

Technical Description
of the Experimental Setup
and Optimization Procedure

Report by Florian Geier

Lund Reports on Atomic Physics, LRAP-386
Lund, July 2007

Acknowledgement

First of all I want to thank Anne L'Huillier for providing me with the opportunity to work on this project and to have a really good time in the Atomic Physics division in Lund. Thanks also go to Miguel Miranda and Xinkui He who have been working with me on this project and did the calculations for the results used in the report. Last but not least do I want to thank the whole division for helping me to enjoy my stay here in Lund.

Abstract

This project was aimed at contributing to the buildup and optimization of the high-order harmonic generation setup in Lund.
The report will therefore give a technical description of the setup and associated procedures, emphasizing the parts which have been changed or newly designed and tested.
Some experimental results, that can be used as a basis point to compare data taken in the future with, will also be presented.

Contents

Chapter 1

Introduction

Note: My work here in Lund was done in a group together with Miguel Miranda and (later) also Xinkui He. I will therefore normally write "we" or "our group" when explaining things.

The high-order harmonic generation setup in Lund was, is and will be subject to a lot of changes.
All the changes have in common that they aim at optimizing the energy and properties of the harmonics generated with this setup.

When I started working with this setup, together with Miguel Miranda, a lot of things needed to be done before we could do any real experiments, from realigning the whole setup to finding and fixing a lot of leaks, to just mention two.
We also noticed quite soon that it was very hard to find anyone who was able to explain how everything really worked, especially the different controllers and connections.
A lot of time had to be spent on learning how to really operate the setup and what needed to be done every time before being able to do any experiment with it.

While learning all that, we changed different parts that we were not satisfied with, like the translation stages for the gas target or the position of one of the turbopumps.
We also inserted new parts that allowed us to speed up certain procedures, like the mirror in the gas target chamber used to watch a small hole where the beam could be cut, or gave us new possibilities to change parameters for our experiments, like the $\lambda/2$-plate and the Brewster-window to change the energy and therefore peak intensity of the incident beam.
We also had to find an easy way to measure the energy of our generated harmonics. For this a protective box for the photodiode was built and had to undergo a number of changes, before finnaly being used in the experiments.

Even the data processing was changed to make things faster and easier. The main part (or somewhat everything) there was done by Miguel Miranda and I will therefore not write too much about those things and leave that to him.

Not only we, but also our instructor Anne L'Huillier noticed (or already knew), that preparing the setup for work took too much time. Time, that could have been spent better if there would have been something like a manual describing how to do things and where to check if something didn't work. Since such a manual did not exist at that time, Anne L'Huillier suggested that I should use my report for that purpose and make life for future groups working with this setup a little easier.
That's why this report will be a little bit different compared to other ones. It is not my intention to explain the theoretical background of the experimental results we got (what has been done in some published papers), but to describe how the setup works and is operated.

You will therefore rarely find any theory in this report (aside from Chapter 2), but a lot of pictures and explanations, as well as some important notes.

This report is meant to be a manual and to help people save time and nerves when using the high-order harmonic generation setup here in Lund.

I will start with briefly explaining the theory behind what we were doing (Chapter 2), before explaining the laser system providing us with a beam and how to do alignments there (Chapter 3).
After this, I will describe in detail the parts used in the high-order harmonic generation setup, along with mounting and alignment procedures there (Chapter 4). The newly inserted or changed parts will be emphasized.
Chapters 5 and 6 will explain how to measure the spectrum and energy of the produced harmonics and also include a few results produced by our group. These results were done in a rather short period of time and, while actually being pretty good, should mostly be used as a reference for future measurements.
I will then draw some conclusions and give a small possible outlook in the last Chapter of this report.

Chapter 2

Theory

The generation of high-order harmonics can be observed when intense laser light interacts with atoms or molecules. Femtosecond pulses are normally required to reach this level of intensity. Atoms and molecules respond extremely non-linear to such strong fields, emitting photons of frequencies which are odd multiples of the frequency of the incident laser field.

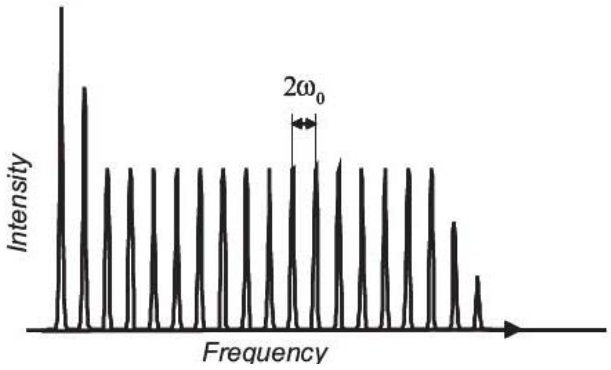

Figure 2.1: A typical spectrum of harmonics

Most spectra of those harmonics look quite similar and can be divided into three parts (as seen in Figure 2.1):

1. The intensity drops with the harmonic order as expected from perturbation theory
2. The intensity stays nearly constant independent from the order of the harmonic
3. An abrupt cut-off occurs

2.1 The Three-Step Model

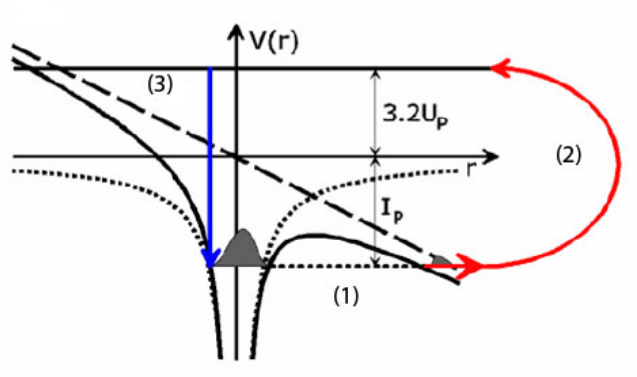

Figure 2.2: The semi-classical three-step model used to to describe harmonic generation

This semi-classical model assumes that an atom only has one electron. The atomic potential is strongly distorted by the electric field of the laser.
This leads to the following three steps which gave this model the characteristic name (see also Figure 2.2):

1. With the electric field of the laser being near the maximum, the electron can tunnel through the barrier provided by the distorted atomic potential.

2. The electron is accelerated away from the atom by the electric field, picking up energy and phase. When the electric field changes its sign, the electron has the possibility to return to the ion core.

3. The electron can recombine with the ion core with a certain probability, emitting the energy gained before as a photon.

The energy gained depends on the phase of the electric field at the time of the emission and of the recombination. The maximum kinetic energy that can be gained by the electron is $3.2U_p$, where U_p is the ponderomotive energy. This U_p is the average energy an electron can gain in an electric field and can be calculated as

$$U_p = \frac{e^2 E_0^2}{4m\omega^2} \tag{2.1}$$

where e is the electron charge, E_0 the field strength, m the electron mass and ω the laser frequency. The maximum energy a photon emitted by a recombining electron can have is therefore

$$E = 3.2U_p + I_p \tag{2.2}$$

with I_p being the ionisation potential of the atom.
Since all the energies up to the maximum energy have approximately the same probability, the plateau in Figure 2.1 occurs.
The explanation why we get discrete harmonic peaks instead of a continuum can also be found in this model: The process of tunneling and recombination occurs twice per laser period T, therefore having a period time $T/2$. That periodicity in time leads to periodicity in frequency of 2ω.
This is however only true for gases and when generating harmonics with a single incident frequency. Using a solid target for high-order harmonic generation or mixing in twice the incident frequency leads to a periodicity of ω. Details for this can be found in the literature.
An electron can actually return to the ion core using one of two different trajectories and still produce a photon of the same energy. These trajectories differ in excursion time of the electron in the continuum and therefore give the emitted light different phases.

2.2 Phase Matching

Very important for harmonic generation is the aspect of phase matching. Phase matching means that the difference in phase between the incident laser beam and the generated harmonic must be minimized to get an efficient energy transfer.
Contributing to the phase mismatch are basically three aspects:

1. Disperion that makes different frequencies travel with different velocities.
2. The Gouy phase shift, inducing a geometrical phase mismatch when a laser beam goes through a focus.
3. The instensity dependence of the harmonic dipole phase.

To explain the concept of phase matching, we consider harmonic generation in a perturbation approximation. The laser field can then be written as

$$E_1(z,t) = \frac{1}{2}[E_1(z)e^{i(k_1 z - \omega t)} + c.c.] \tag{2.3}$$

This field propagates in the medium and generates the second harmonic. The non-linear polarization becomes

$$P_2^{NL} = \epsilon_0 \chi^{(2)} E_1^2 = \epsilon_0 \chi^{(2)} [E_1^2(z) e^{i(2k_1 z - 2wt)} + c.c]. \tag{2.4}$$

where $\chi^{(2)}$ is the 2^{nd} order susceptibility of the medium. The emitted radiation has a new wave vector k_2 and a frequency 2ω. The electric field for this is

$$E_2(z,t) = \frac{1}{2}[E_2(z)e^{i(k_2 z - 2\omega t)} + c.c.] \tag{2.5}$$

Comparing polarization and generating field, we can conclude that they will propagate with different phase velocities if there is a mismatch in the wave

vectors. This phase mismatch $\Delta k = k_2 - 2k_1$ has to be minimized in order to get an efficient energy transfer from the laser to the harmonic. The consequences of a lack of phase matching can be seen in Figure 2.3.

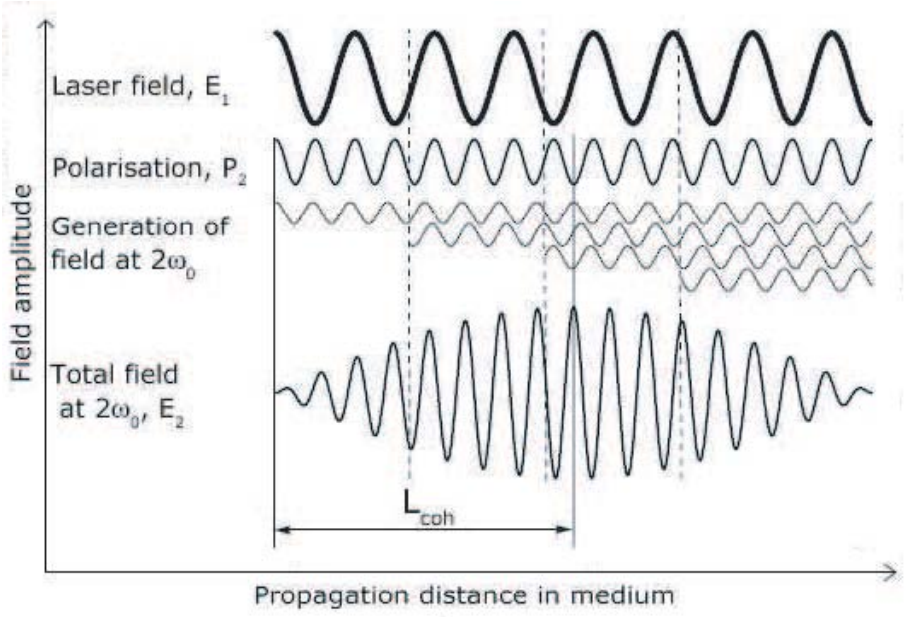

Figure 2.3: The effects of a phase mismatch

A parameter used to characterize the phase matching is the coherence length L_{coh}, which is the distance for which the field is built up constructively. L_{coh} is given as

$$k_2 L_{coh} - 2k_1 L_{coh} = \pi \tag{2.6}$$

leading to

$$L_{coh} = \frac{\pi}{\Delta k} \tag{2.7}$$

Both trajectories contribute to the harmonic dipole moment with a term characterized by a phase Φ_i given by

$$\Phi_i = -\alpha_i I(z) \tag{2.8}$$

The intensity dependence of the phase leads to a spectral broadening and chirp of each harmonic. The α_i is different for short and long trajecotry and related to the time the electron spends in the continuum.
Spectral content and chirp of the harmonic differ depending on the dominant trajectory. The intensity varies over the pulse temporally and spatially. Radial variation $I(r)$ will affect the curvature of the harmonics phase front. The short trajectory will therefore be associated with a smaller divergence, the long with a larger one.

The total electric field of the harmonics is written as

$$E = E_l e^{-\alpha_l I} + E_s e^{-\alpha_s I} \tag{2.9}$$

With E_l and α_l being the electric field and α-value for the long trajectory, E_s and α_s for the short one.

Chapter 3

The 10 Hz Multi-Terrawatt Laser System in Lund

This chapter is dedicated to explaining how the 10 Hz multi-terrawatt laser system in Lund works and how to align the parts needed for work with the high-order harmonic generation setup.

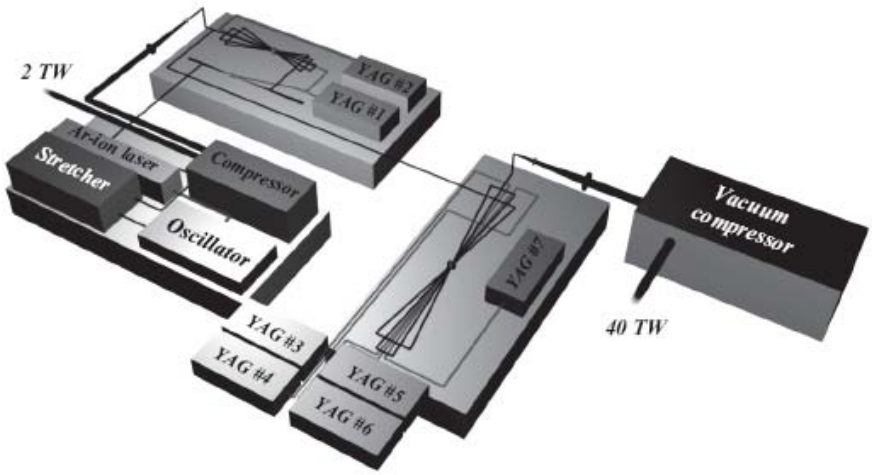

Figure 3.1: A scheme of the 10 HZ multi-terrawatt laser system, the amplifier pumped by YAGs 3-7 is not used for the HHG beam line

The laser providing us with the beam for experiments is a Ti:Sapphire system operating at 800 nm. The laser pumping the cavity is a Spectra-Physics

Millenia V, the inital pulse runs a certain number of passes through an oscillator and is then sent to a stretcher.
The stretching is necessary to be able to amplify it without damaging the amplifiers.
The pulse passes through a butterfly amplifier pumped by two YAG lasers and is therefore amplified several times before being compress again down to about 40 fs pulselength with a pulse energy of up to ≈200 mJ before compression.
This procedure is known as chirped pulse amplification.

To operate the high-order harmonic generation setup (called HHG setup from now on), the beam's path through the compressor has to be aligned each time experiments are done.
It is recommended to do the alignment procedure with a reduced pulse energy to ensure the safety of the working persons. To reduce the pulse energy by approximately a factor of ten, simply change the delay of one of the YAG pumping the amplifier (YAG #2) at the master clock run by the main computer in this room (higher the pump delay by 0.1 by just pressing the "up"-button once) (see Figure 3.2).
Since changing the delay will also affect the second beam line used in another room, check with the people there if they need the highest possible pulse energy at the moment or not.
After the alignment is done, change the pump laser back to how it was before.

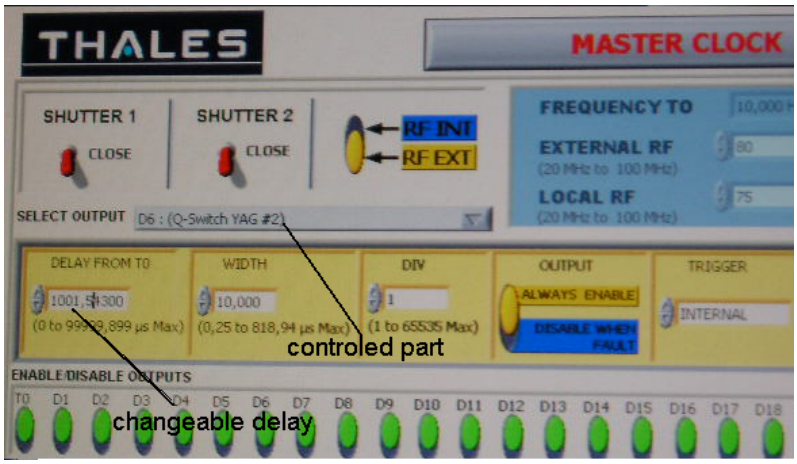

Figure 3.2: Master clock screen on the computer

Two mirrors are used to align the beam's path through the compressor. These mirrors can be seen in 3.3.
The beam is normally blocked before these two mirrors due to safety reasons. A control box (see Figure 3.4) is installed to change the properties of the blocking.

Figure 3.3: The two mirrors in front of the compressor

The switch of this box should be in the middle position when experiments are done with the HHG setup, because the blocking can then be remotely controlled from the other room. The left position means "always blocked", while right means "never blocked".
The remote control will only work when the tube (see Figure 3.4) is in place, closing the two contacts after the mirrors mentioned above.

Figure 3.4: The control box for the blocker before the alignment mirrors and the tube used between the mirrors and the compressor

Important points to check the alignment are two irises, seen in Figure 3.5. The alignment is therefore done as following:

1. Close the first iris until you can see if the beam passes symmectrically or not. If it does not, tilt the first mirror until it does.
2. Open the first iris completely and check with the second iris (directly before the wall) if the beam passes through symmetrically. Tilt the second mirror until it does if needed.
3. Check with the first iris again, since tilting the second mirror may have changed the path there. Use the first mirror to correct the path.
4. Check with the second iris again, use the second mirror if needed.
5. Repeat this as often as needed until the beam passes symmetrically through both irises. Now open them both, so you can use the beam in the other room for the HHG setup.

To easily change the energy of the pulse before compression and with that the peak intensity used in the HHG setup, a $\lambda/2$-plate and a Brewster-window have been inserted by our group. The $\lambda/2$-plate is used to change the rate of polarisation that is being transmitted by the Brewster-window.
When using these parts, some light is being reflected downwards from the Brewster-window. This light should be blocked due to safety reasons. A black box (see Figure 3.6) has been built for this and can be put over the Brewster-window. Figure 3.6 also shows the newly inserted parts.

By simply rotating the $\lambda/2$-plate, the pulse energy can be varied. To check the pulse energy, use the powermeter standing near the mirrors.
The maximum achievable energy is not absolutely constant due to the different quality of alignment for the laser each day.
Normally the maximum energy should be between 170 mJ and 200 mJ before compression.
In our experiments the energy before compression was set to a value of 150 mJ every day to not be influenced by the maximum energy of the corresponding day.

Note: Should the $\lambda/2$-plate and/or the Brewster-window not be in place, they will most likely be used in the Attolab. Check with the people there if they really need them or if they can be borrowed for the duration of the experiment. The parts can be inserted and taken out very quickly.

Another way to change both the peak intensity of the pulse and the pulse duration (along with other parameters) is to change the grating position inside

Figure 3.5: The compressor, parts important for the alignment have been labeled

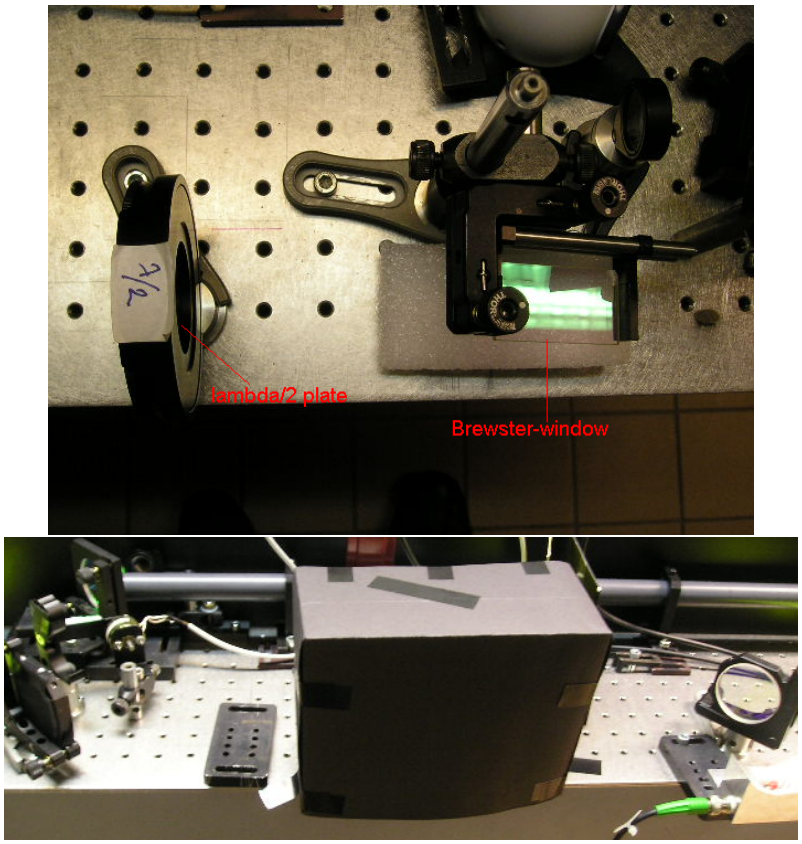

Figure 3.6: The newly inserted $\lambda/2$-plate and Brewster-window to change the energy of the incoming beam + the black box to block reflected light

the compressor. Figure 3.5 shows the two compressor gratings and Figure 3.7 the screw that can be used to change their position.
To get the lowest possible pulse duration (around 40 fs), the gratings have to be placed in a position called "zero position" that has to be found by using autocorrolation.
We found this position to be around 10.2 μm.

Note: Be careful not to touch the gratings! Direct contact will destroy their surface.

A combination of polarizer and gratings can be used to only change the chirp while having a constant peak intensity if needed.

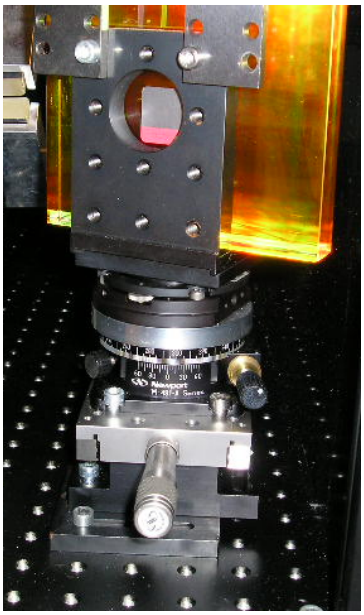

Figure 3.7: The screw used to change the position of the gratings in the compressor

Note: If you should see a beam at the first iris, but no beam at all at the gratings and the second iris, it is possible that the compressor has been set for one-shot-experiments (sometimes used for the other setup in the room of the HHG setup). There will then be a beam dump in the compressor that needs to be removed. The beam dump can be seen in Figure 3.5.

Chapter 4

The High-Order Harmonic Generation Setup

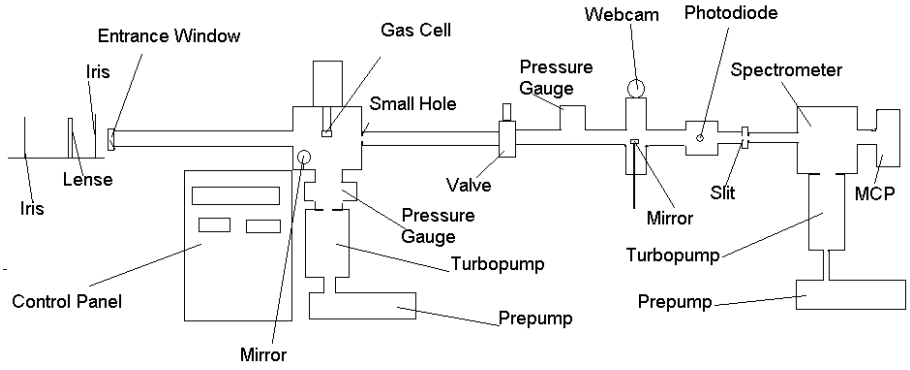

Figure 4.1: A scheme of the setup used in the experiment

Figure 4.1 shows a scheme of the HHG setup used for the experiments. The beam provided by the system that is described in Chapter 3 is reflected by two mirrors which are used for alignment purpose (described later in this chapter), cut by an iris and then focused by a lens with a focal length of 2 m. After this an entrance window into a vacuum chamber is passed. This is necessary because from there on everything has to be kept under vacuum. The major reasons for this are:

1. To avoid ionisation of the air due to high peak intensities in the focused beam
2. To enable XUV light to travel long distances without significant absorption

3. To be able to operate the MCP (see Chapter 5)

Here are some typical numbers for the pressure inside the setup after pumping for several days:

position	pressure with gas closed	pressure with gas pulsed
gas target chamber	7×10^{-7} mbar	10^{-5} up to 10^{-4} mbar
after the valve	2×10^{-6} mbar	up to 2×10^{-5} mbar

Before our work, the second vacuum pump was connected to the pressure gauge behind the valve with a tube of ≈ 3.5 cm diameter. With this a pressure of $\approx 5 \times 10^{-5}$ mbar registered at the gauge was reachable. Due to some leaks between the gauge and the MCP, the real pressure at the MCP was actually higher than that.

Connecting the pump directly to the spectrometer using a tube of 10 cm diameter enabled us to get a vacuum registered at the gauge in the low 10^{-6} mbar region when the gas is closed and low 10^{-5} mbar region when gas is allowed to flow in. The pressure at the MCP is furthermore lower than the registered one, because there are some possibilities for leaks close to the gauge, but quite far away from the pump and MCP. There should be no significant leak possibilities between the pump and the MCP.

Typical leak points that have been found and fixed as good as possible are:

- The entrance window, where the beam enters the vacuum chamber
- The pressure gauge after the valve
- The adjustment pole for the mirror to watch the slit
- The window for the webcam
- The construction containing the adjustment pole for the photodiode, the electrical contacts for it and so on

Our gas target is placed at a distance of 2 m from the lens.

4.1 The Gas Target

The gas cell we are using was designed by Tobias Eberle and Jan Klemmer in 2006 [2] and replaced the old system which used a gas nozzle (shown in Figure 4.2).

Figure 4.3 shows a scheme of the cell and Figure 4.4 how the cell looks when mounted.

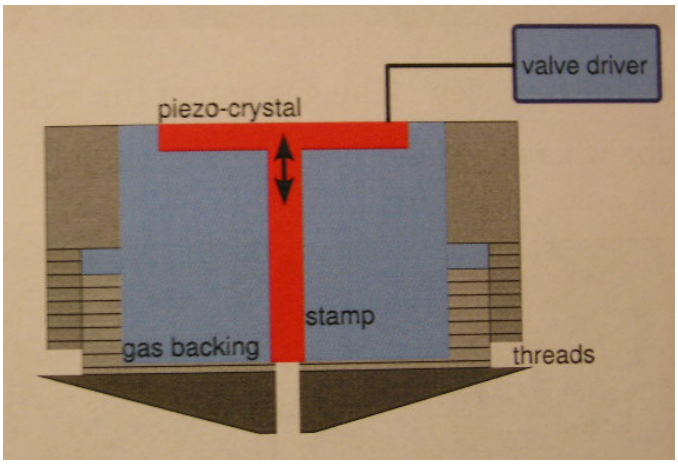

Figure 4.2: The old gas system - the nozzle was recently replaced by the new gas cell

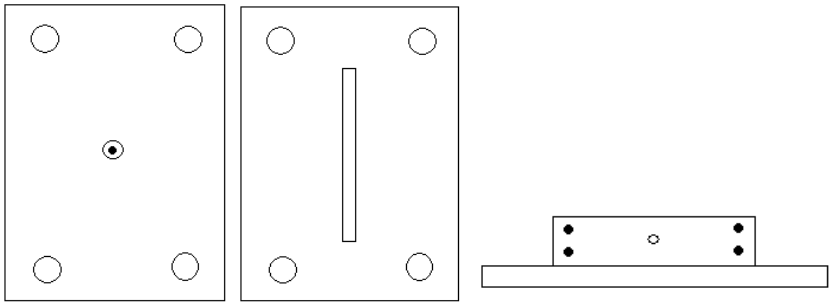

Figure 4.3: Scheme of the gas cell used, pictures are (left to right): bottomview, topview, sideview

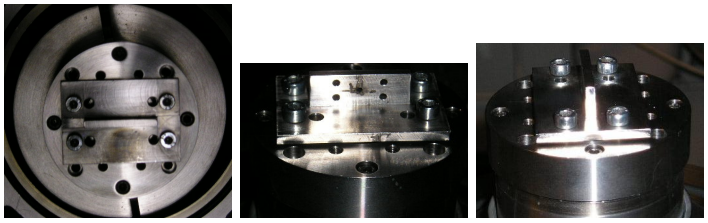

Figure 4.4: The cell when mounted, seen from different points of view

The cell is still being filled with argon gas (like the nozzle) at a 10 Hz repetition rate by a piezo crystal.
The gas bottle needs to be opened before working with the target. To do so,

turn the handle directly at the bottle in the "open" direction (written on the handle) as far as possible. Then turn the red handle at the pressure gauge slowly until a pressure of ≈1 bar is displayed.
Gas can now stream into the buffer storing it before reaching the piezo crystal. The controller for the gas buffer can be seen in Figure 4.5.

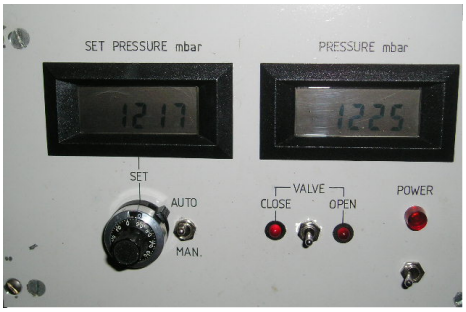

Figure 4.5: The controller for the gas buffer

When the left switch is set to "auto", gas will be allowed to flow in (placing the right switch on "open") until the "set pressure" value is reached. As soon as this happens, the gas buffer will shut the gas stream off and only open again if the real pressure drops below the set value.
Should the controller be damaged and/or not working properly, the left switch can be set to "man" and the right one to "open". This will allow gas to stream into the buffer and to the piezo crystal all the time. To not damage any parts, the pressure has to be controlled directly at the gas bottle in this case. The pressure at the gauge next to the bottle should then be set to ≈0.5 bar. Because this gauge shows the difference between inside and outside pressure, this is equal to ≈1.5 bar reachable in the buffer, which is a reasonable value for experiments.
The trigger for the piezo crystal is being provided by the terrawatt system. To enable the 10 Hz pulsing, connect the "input" port of the piezo controller to the trigger cable coming from the laser system. The "trig out" port should be connected to to CCD camera (see Chapter 5) and the "output" port to the piezo crystal.

The "sync" port can be connected to an oscilloscope to check pulse duration and voltage if needed. This port sends a signal equal to the one sent by "output", lessened by a factor of ten. The pulse width and voltage can be changed at the piezo controller. The maximum voltage achievable from the controller has been turned down from 230 V to ≈120 V. This is the typical working voltage for the crystal and it is therefore recommended to always use this value.
The reason why the controller is originally produced for a voltage of 230 V is

that the piezo crystals used before needed a higher voltage to work properly (up to 230 V).

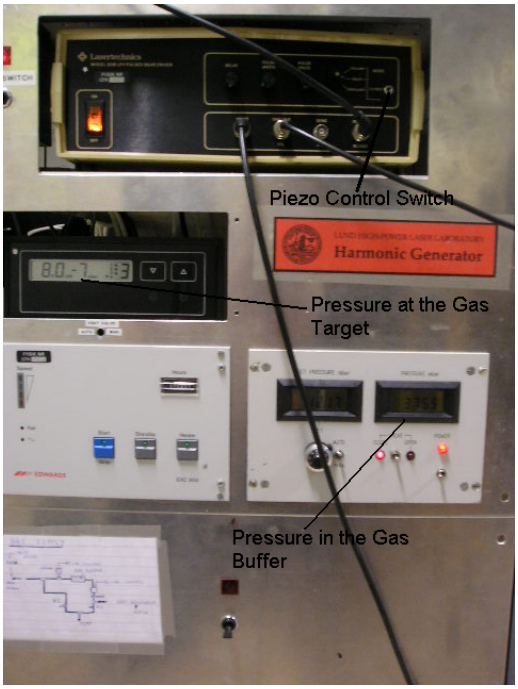

Figure 4.6: The control panel with the controller for the piezo element, a display for the pressure under the cell chamber and a controller for the gas buffer

Figure 4.7: A detailed view of the piezo controller

The switch is used to control the gas flowing into the cell:

switch position	effect
downmost	pulsed, repetition rate of 10 Hz
middle	closed, no gas should flow into the cell
uppermost	open, gas can flow in continuously

Note: Never put the switch of the piezo controller in the uppermost position! This will allow the gas to stream into the setup constantly and may (and most likely will) lead to an overload of the turbo pump.

The length of the cell can be varied from 3 mm up to 25 mm by adding metal plates of length 1 mm, 2 mm and 4 mm.
The four 4 mm plates have been built recently to be able to do experiments with cells longer than 9 mm, what was the limit for the original cell.

When mounting the cell, certain things have to be considered. The procedure is explained in the report of Tobias Eberle and Jan Klemmer, but a few new things were found out recently:
After the cell has been mounted, you can either try to feel the pressure of outcoming gas to see if there are leaks/if the gas is coming out when pulsing the piezo element, or you can use another procedure:
Mount the whole device with the cell and start pumping the chamber (using the prepump should normally be enough) and set the controller for the gas buffer to "man" and "closed", so that no new gas can flow into the buffer to compensate for leaks. After reaching a pressure of around 10^{-1} mbar, check if the pressure in the gas buffer (can be seen at the controller in Figure 4.6) is going down and, if yes, how fast it is.
When having the piezo crystal in the closed position, there should be no decrease (or a decrease of 1 mbar at a time). Should there be more, you won't be able to get a vacuum of 10^{-5} mbar or less because of leaks. When pulsing the piezo crystal, there should be a considerable decrease of pressure in the gas buffer ($\geq$ 4 mbar at a time). This indicates that there will be enough gas coming out to have harmonics created.
Should these requirements not be fullfilled, stop the prepump, take the cell off and screw or unscrew it a little, then try again.
This may take a few tries, but should still be faster than working with the turbopump to check the maximal reachable vacuum.

When the cell is mounted correctly, start the prepump, wait until a vacuum of $\approx 10^{-2}$ mbar is reached and start the turbopump. A pressure in the 10^{-6} mbar region should be reached after a few hours.

With this pressure you can open the valve without risking damage to the MCP

by destroying the vacuum on its part.

The valve should be closed when not doing experimets to guarantee the safety of the MCP in case the pump near the gas target malfunctions.
The part of the setup after the valve should be under vacuum at all times and may only be flooded with air when the setup has to be changed there.

After the cell, the incident beam together with the harmonics travels some more distance before it can either be detected by a photodiode or be directed through a 200 μm slit to the spectrometer.

4.2 Alignment

After the beam's path is aligned with the compressor and the gas target mounted, it needs to be aligned with the HHG setup shown in Figure 4.1.

Two mirrors in the HHG room (shown in Figure 4.8) are used for that purpose.

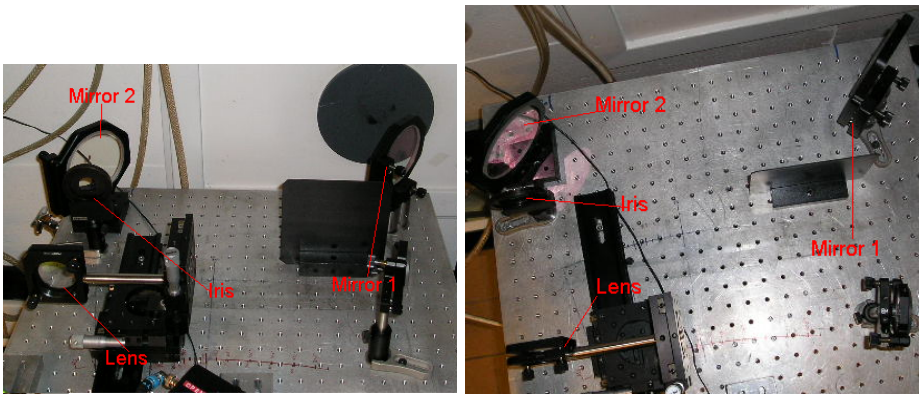

Figure 4.8: Mirror 1 and Mirror 2 are used to align the beam through the whole setup, the lens can be removed for alignments

Critical points in the setup are:

- The iris behind the two mirrors
- The small hole after the gas cell, where the beam has to pass through
- The slit before the spectrometer

Take the lens out and align the beam without it:
The first mirror situated directly after the hole in the wall should be used to make the beam pass through the iris symmetrically.

A small mirror has been implemented in the chamber, where the gas target is situated, that allows you to watch the small hole at the end of the chamber without having to force your head into unnatural positions. Adjust the second mirror until the beam passes through the hole and is not cut by the walls. Now use the webcam to see if the beam hits the slit in front of the spectrometer. You may need to turn on the lamp next to the camera to be able to see a clear picture on the computer screen. Reduce the beam size by closing the iris until you only see a small spot and check if this spot directly hits the slit. If it does not, tilt the second mirror until it does. Normally adjusting by watching the hole in the gas cell chamber or the slit should automatically align the other one, but check each time to be sure.
Now put the lens back in and check if the beam is still aligned. If it is not, try tilting and moving the lens by using the translation stages connected to it. The alignment of the beam is finished as soon as you manage to hit the slit with the lens being in place.

It is now time to align the gas target:
Lower the target by using the translator on top of the holder (shown in Figure 4.9).

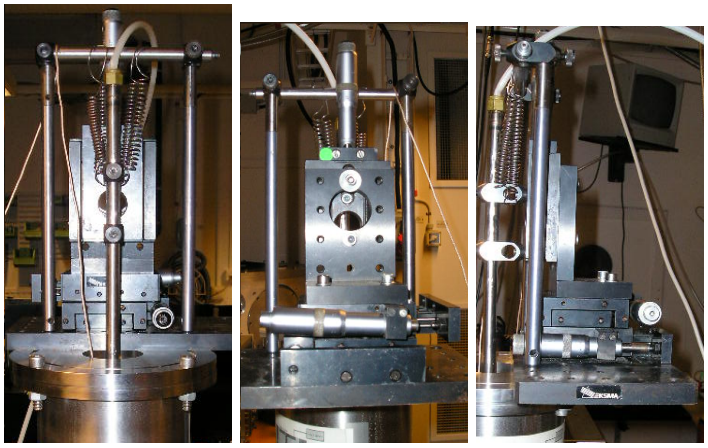

Figure 4.9: The translation stages to move the gas target

Four springs have been added to this translation stage to enable a normal person to screw it manually. Without those screws, the force pulling the target down (due to the pressure difference inside and outside of the chamber) is too much for the translation stage to handle and it will be damaged.

When using the old gas nozzle , lower it until you see the beam hitting the nozzle itself and lift the nozzle up a little bit so the beam is then situated directly under it. Now open the gas bottle and set the pressure at the bottle to around 1 bar. Set the pressure at the control panel to around 1.2 bar and the controller for the piezo crystal to pulsed (lowermost position).
By using the lowermost of the three translation stages connected to the gas target, move the nozzle perpendicular to the beam until you can see a bright spark. Turn off the gas by putting the switch on the piezo control box to the middle position.
If the spark disappears, everything is fine and the nozzle is aligned. If the spark is still there, your beam is hitting the nozzle and you will have to lift it up a bit to avoid this.

When using the new gas cell , lower it until you can see the beam hitting the approximate location of the hole, where it should pass through. If needed adjust the cell perpendicular to the beam by using the lowermost of the three translation stages. When the beam is going through the small hole, turn on the gas by putting the control switch for the piezo crystal into the lowermost position. You should now see a bright spark that disappears when you turn of the gas.

Note: The mirror situated in the chamber of the gas target can be used to check where the beam hits the target. Use a flashlight to see everything more clealy if needed.

Note: The second translation stage can be used to move the target along the beam line. It is however recommended not to use it, because the target may tilt.
If you want to change the position of the target out of the direct focus it is easier to move the lens instead.

The alignment procedures for the spectrometer and photodiode will be discussed later in this report (Chapters 5 and 6).

Chapter 5

Measurement of the Spectrum

To measure the spectrum, the photodiode needs to be moved out of the beam. This is done by simply pulling the adjustment pole out as far as possible and fixing it in that position by tightening the screw on it.

The beam will now be able to hit the 200 μm slit and then enter the spectrometer.

5.1 The Spectrometer

The I.S.A. Jobin-Yvon PGM PGS 200 spectrometer used works as following:

- A toroidal mirror focuses the beam on a XUV grating.
- The plane platinum coated grating with 450 grooves/mm is designed for a spectral range of 16-80 nm and separates the different wavelengths.

The grating can be rotated to see different parts of the spectrum. This is done by either turning a controller directly at the spectrometer (see Figure 5.1, only a very small rotation range is possible there) or by using the control box on the table (see Figure 5.2).
The switch on this box can be turned up or down to tilt the grating in either direction. By turning the switch up/down further, the rotation can be done faster.
The buttons on the right side of the control box can be used to set the desired position for the grating.
After pressing the "run" button, the grating will automatically be moved to this position.

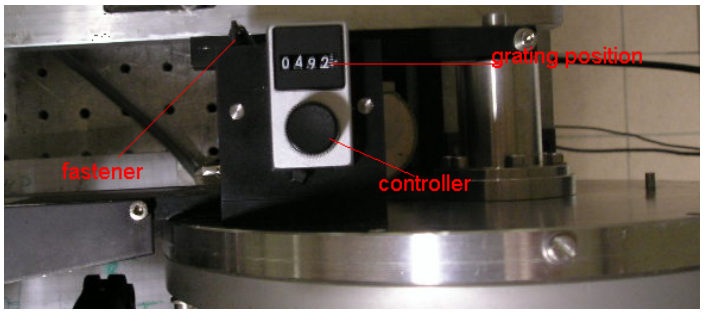

Figure 5.1: The controller for the grating, the display of the real grating position and the grating fastener

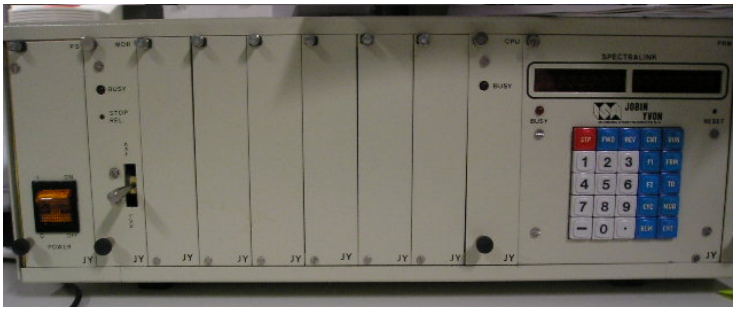

Figure 5.2: The control box for the grating

The position shown at the controller does however not have to be the same as the real grating position. The real position can be seen near the controller in Figure 5.1.

Note: The fastener has to be in the position shown in Figure 5.1. The rotation of the grating will be blocked, should it be in any other position!

Note: Should the spectrum seen be asymmetric, the spectrometer may need to be aligned. This can be done by moving the table it is situated on a bit or tightening the screws fixing the spectrometer on the table to tilt it.

5.2 The Micro-Channel Plate

The micro-channel plate consists of an array of $10^4 - 10^7$ electron multiplier channels, oriented parallel to each other and having a diameter of $10\,\mu$m. Electrons are created when XUV photons hit the surface. These electrons are accelerated and multiplied by collisions with the walls of the channel. After this amplification, they are made visible by a phosphor screen. The typical

voltages used at the MCP are +3000 V at the phosphor screen and -1500 V at the surface situated closest to the spectrometer.
In order to use the MCP a pressure of less than 10^{-5} mbar has to be guaranteed and at startup the voltages should be increased in steps of 100 V with some pause (around 1-2 minutes) between each step.
Care must also be taken not to switch the sign of the voltage, since doing so and applying a high voltage would destroy the MCP with a very high probability. When using the MCP for the first time after having it exposed to air, the startup procedure should be done very carefully and with smaller steps and longer pauses in between. To be absolutely sure the procedure described in the manual can be used, though it will then take at least 4-5 hours to get ready.

A higher voltage difference can be used for the MCP to see a brighter spectrum. This will however also increase the level of noise significantly. While the 3000 V at the phosphor screen should be kept constant, the other voltage can be changed up to 2000 V.

5.3 The CCD-Camera

The picture of the MCP's phosphor screen needs to be taken and stored in order to get data about the spectrum. For this we used a Charged-Coupled device (CCD) camera, type Marlin F-033B/C with 656×494 pixels.
The camera is connected to the computer in the lab via a firewire cable.
A LabView program was written by Miguel Miranda to read out the data from the camera and directly process in to a certain degree in order to be able to draw some conclusions about the spectrum's properties.

Note: It is possible that the camera driver is not installed on the computer. If this should be the case, open *My Computer* → *Properties* → *Hardware* → *Device Manager* and install the NI-IMAQ driver for the camera manually.

The camera was formerly attached to a large metal pole in order to guarantee its stability. This and the fact that the translation stage of the camera was damages, made a fast and precise alignment nearly impossible.
It was also very hard to move from one side of the setup to the other without touching the pole and therefore destroying the camera alignment.

This was changed by fixing the camera to the table the spectrometer is placed on. This and using a new translation stage helps to align the camera correctly and keep the alignment over a longer period of time.

5.4 Experimental Results

A typical spectrum recorded as raw data and later plotted in Matlab looks like shown in Figure 5.3.

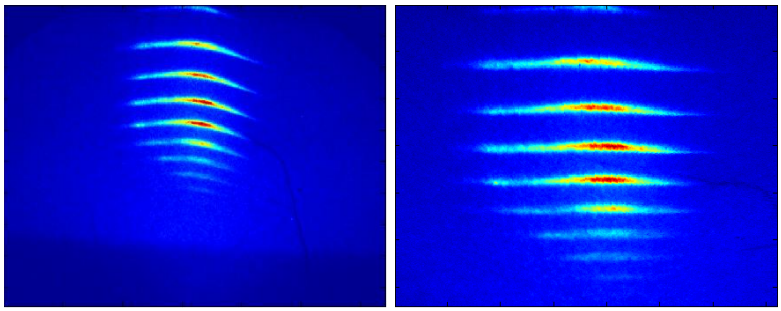

Figure 5.3: A typical spectrum before and after straightening

To be able to work with the data, the spectrum needs to be changed fom the curved lines seen in Figure 5.3 to straight ones. This is done by finding the function representing the circle representing the harmonic and rearranging the data using this function.

All the spectra shown in this report from now on will already be straightened to ease their understanding.

In these straightened spectra, the x-axis represents divergence, while the y-axis represents wavelength.

Some measurements were done to see the difference in the spectrum when using the new gas cell instead of the old gas nozzle:

When using the nozzle , the intensity of the spectrum is relatively low, but under certain conditions (namely a sufficient peak intensity) multiple peaks for each harmonic can be seen (representing the short and long trajectory). Two peaks for the stronger harmonics are normally able to be seen, sometimes even three.(see Figure 5.4).

When using the cell , the intensity of the spectrum was considerably higher, but the multiple peaks were either gone (for long cells >9 mm) or very weak (shorter cells and/or optimized input energies).

In our other measurements did we vary the diameter of the iris behind the two adjustment mirrors for the HHG setup und therefore changed the input energy and beam diameter in the focus.

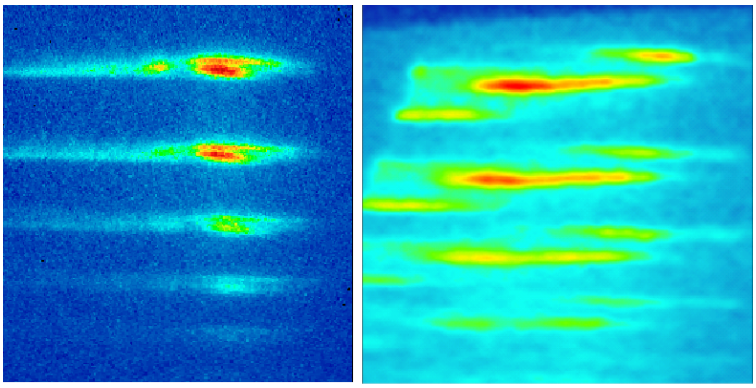

Figure 5.4: Spectra with double peaks (left) and triple peaks (right) recorded when using the nozzle

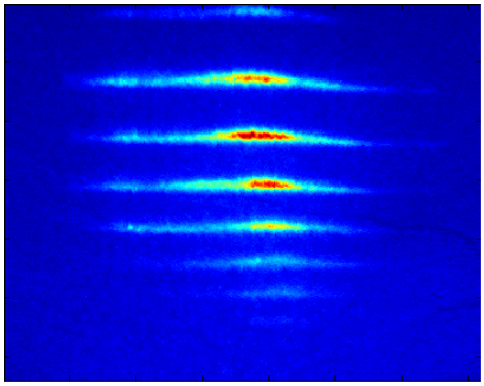

Figure 5.5: Spectrum for the cell not showing multiple peaks even when using high input energies

The energy values for the incident beam for different iris diameters are given in the following table. The energy before compression used was 150 mJ.

iris [mm]	10	11	12	13	14	15	16	17	18	19	20	21	22	23
energy [mJ]	4.5	5.3	6.0	6.8	7.9	9	10.9	12.8	14.6	16.5	18.8	21.0	22.9	24.8

The pressure was set to 1.2 bar in the gas buffer for every measurement. The real pressure in the cell is unknown and can not be measured easily. It has hower been shown in [2] that the generated harmonic intensities are independent of the gas pressure when using the cell.

Data for the different iris diameters mentioned above was taken for different cell lengths, varying from 9 mm up to 19 mm.
A typical series of spectra is shown in Figure 5.6.

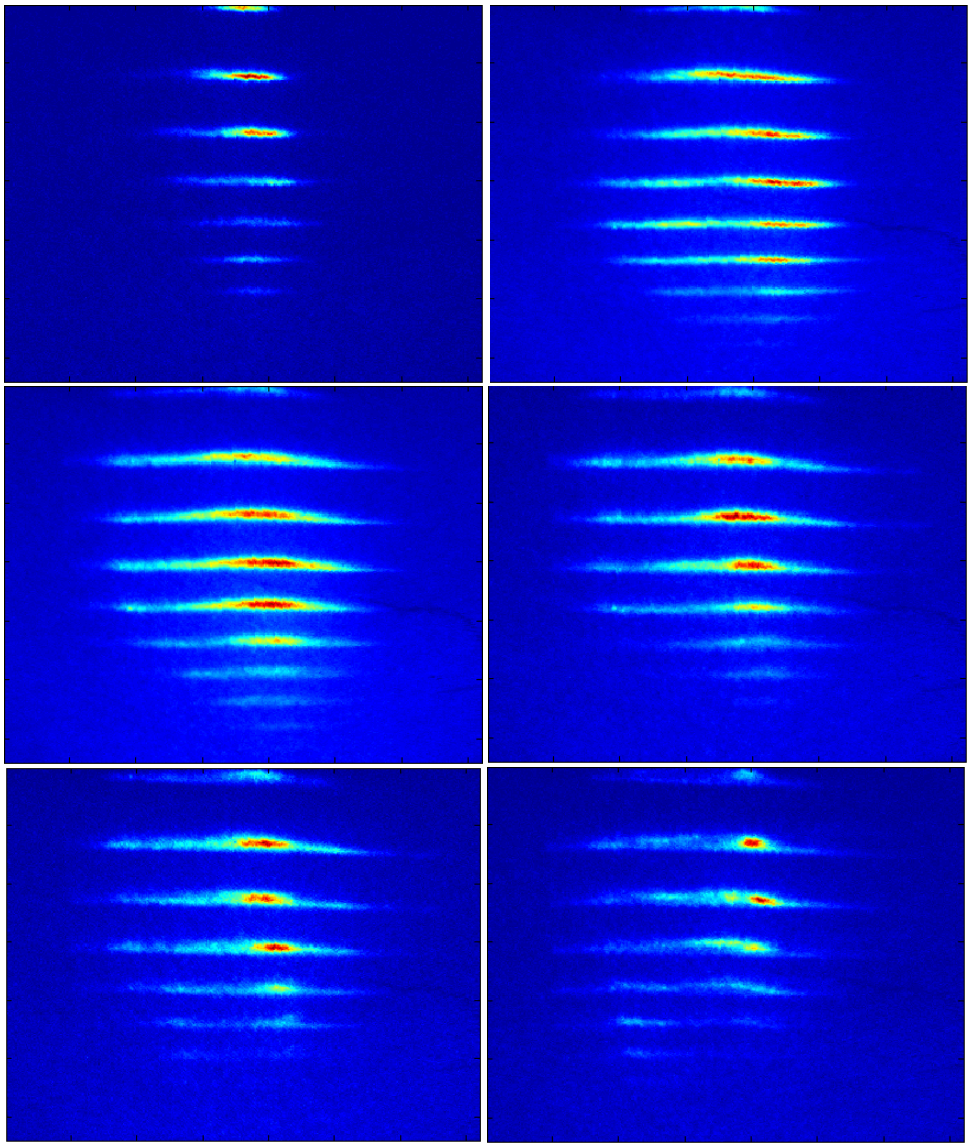

Figure 5.6: Typical series of spectra, here for iris diameters (from left to right) 11 mm, 12 mm, 14 mm, 16 mm, 17 mm and 18 mm and a 15 mm cell using 150 mJ input energy before compression, 1.2 bar and 40 fs pulses

The most intense spectra were recorded with the longest cell used in the experiments (19 mm). The optimum seemed to be at around 20 mm iris diameter. This spectrum can be seen in Figure 5.7.

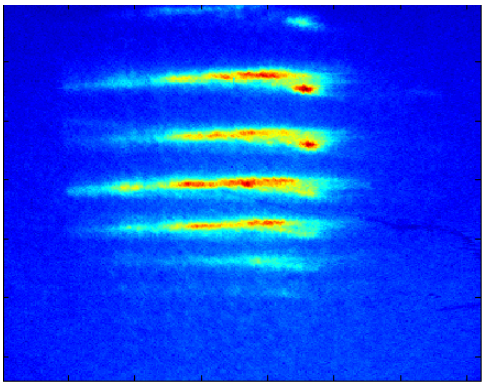

Figure 5.7: Most intense spectrum recorded, using 20 mm iris diameter, 19 mm cell length, 150 mJ input energy before compression, 1.2 bar pressure and 40 fs pulses

With the 19 mm cell, it was also clearly seen that the spectrum seems to start with a distinct intensity peak in each harmonic and gets a flatter intensity distribution when having higher overall intensity (when using larger iris diameters). After passing a certain point, a sharp intensity peak seems to build up again, moved to the left side compared to the original peak.
This development can be seen in Figure 5.8.

It is not completely clear why a new peak forms after a certain level of input energy is reached and why this peak is moved to one side.
It may be possible that two new peaks, one to either side, do in fact form and one is clipped by some part of the spectrometer. The two peaks could then maybe be explained with being the intensity maxima of the long trajectory, while the original one peak in the middle of the spectrum was the intensity maximum of the short trajectory.
It could also be an effect of disalignment.

With the spectra recorded and straightened, we integrated along the divergence axis and got the pure frequency dependent intensity spectrum for each measurement (a typical one seen in Figure 5.9).
When comparing some of those spectra, we could see that the FWHM of the harmonics gets larger when increasing the iris diameter, as seen in Figure 5.10.

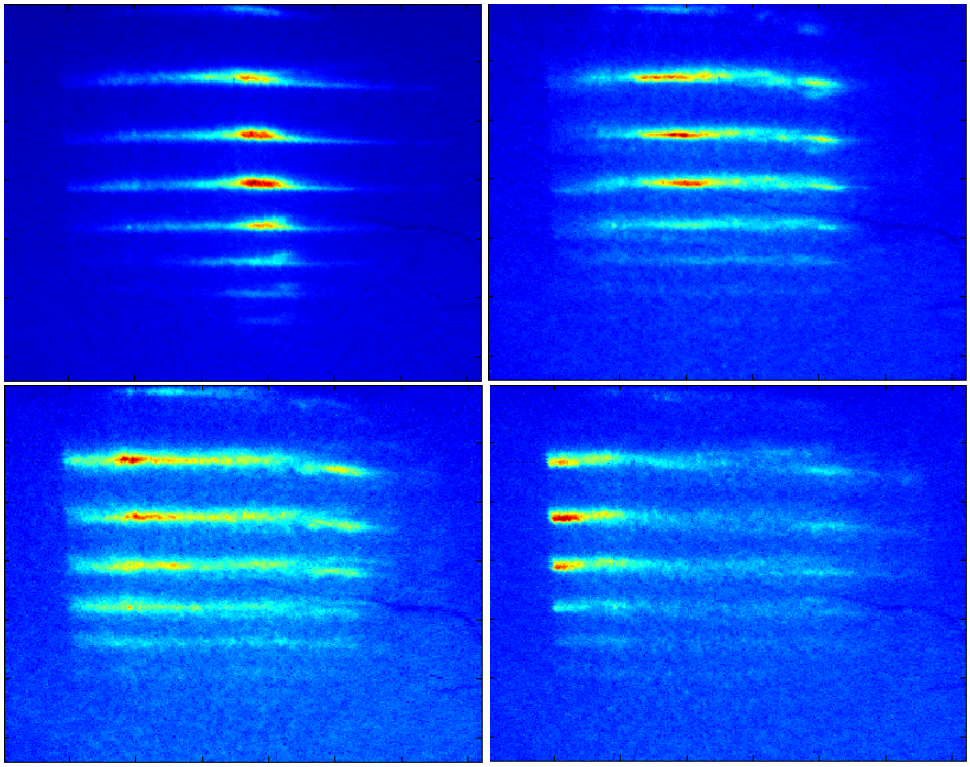

Figure 5.8: Spectra for (from left to right) 16 mm, 22 mm, 24 mm and 28 mm iris diameter, 19 mm cell length, 150 mJ input energy before compression, 1.2 bar pressure and 40 fs pulses

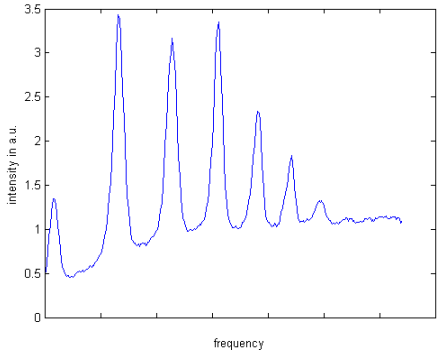

Figure 5.9: A typical spectrum for relative intensities of the harmonics before averaging and interpolating, here for 15 mm cell length and 17 mm iris diameter, 150 mJ input energy before compression, 1.2 bar pressure and 40 fs pulses

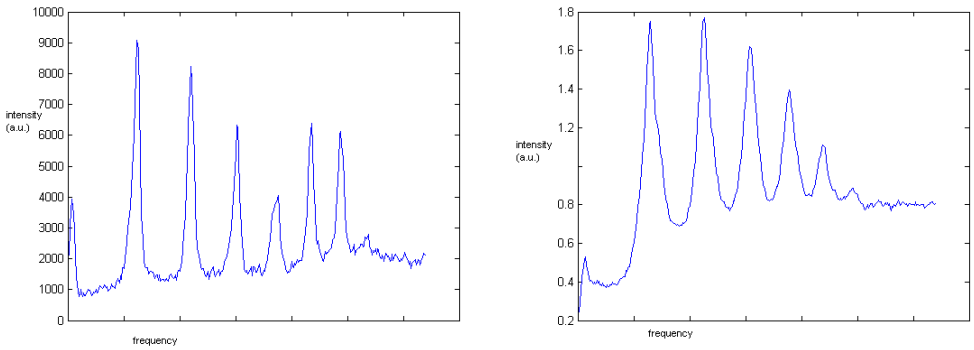

Figure 5.10: Harmonic spectrum for 11 mm iris diameter (left) and 24 mm iris diameter (right) for a 19 mm gas cell, 150 mJ input energy before compression, 1.2 bar pressure and 40 fs pulses

Chapter 6

Measurement of the Energy

A photodiode has to be placed in the beam line to measure the energy of the generated harmonics.

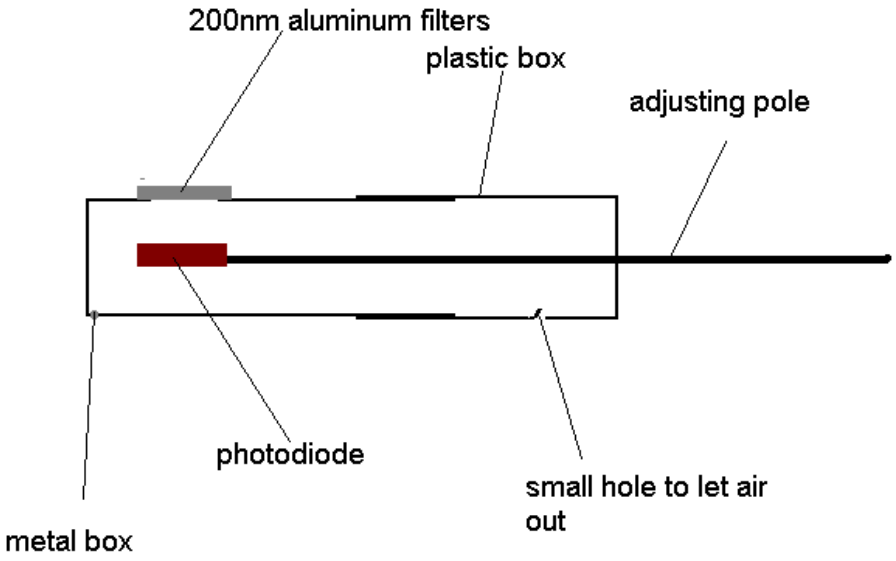

Figure 6.1: Scheme of the box containing the photodiode

Figure 6.1 shows a scheme of the box which was used to mount the photodiode. How the box looks in reality can be seen in Figure 6.2.
The photodiode can be moved into and out of the beam rather easily by just pushing/pulling on the metal holder (see Figure 6.3). As soon as you are sure the beam hits the filters, you can try turning the adjusting pole and optimize

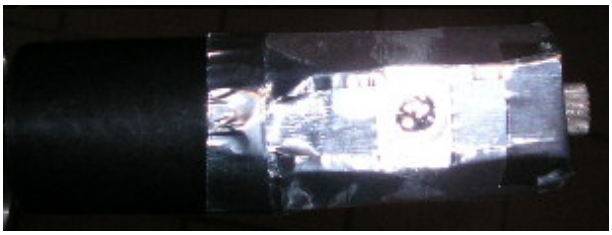

Figure 6.2: The box containing the photodiode

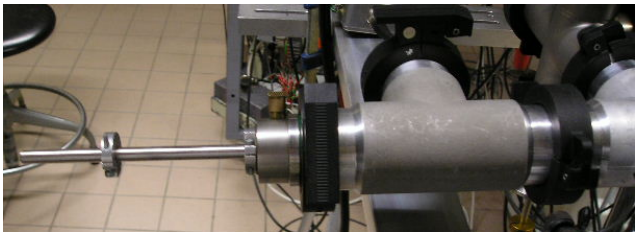

Figure 6.3: The holder of the photodiode allows to move it in and out very easily

the signal registered by the diode this way.
The webcam can also be used to check where the beam hits the box of the photodiode.
Two aluminum filters of 200 nm thickness each had to be used to block enough of the incident beam to not have any signal while no harmonics were generated and to avoid saturation even with a relatively low harmonic signal.

We consider our filters to be exactly 200 nm thick, but this value may differ by a few nm in reality.
The filters are assumed to be pure aluminum and oxidation effects are not considered when doing the calculations later on. It was however shown experimentally that a 200 nm filter can be considered to be around 185 nm pure aluminum and 15 nm aluminum oxide [4].
This changes the transmission function significantly and leads to a way smaller energy registered by the photodiode.
Because our calculations are done with the transmission function for pure 200 nm aluminum, our calculated energy values will be significantly lower than the real ones.
We also assume that the harmonic beam is not cut by the filters and enters the box with its full diameter. It is possible and somewhat likely that a part of the beam may not be hitting the transitive part of the filters, but instead the part where the filters are mounted on metal rings to guarantee stability.
A small part of the diode is furthermore damaged and may not register any

signal at all.
We do therefore most likely register only a part of the generated harmonics, meaning that our calculated values are even further below the real ones.

Our first idea was to mount the filters by clamping them to the box with screws. This failed due to the fact that the screw holes would let stray light into the box, leading to a saturation of our photodiode. This problem was solved by using multiple layers of special tape (usable under vacuum conditions) instead.
When using only the filters to block out incoming light, stray light would still saturate the diode and render us unable to get any reasonable results. For this a combination of a near cylindric metal box, a cylindric plastic box and tape to cover smaller openings was used. Tests were performed to locate the direction of incoming stray light and needed isolation and the results showed that only a covering in every direction could provide a sufficient protection from stray light to allow us to perform measurements.
A small hole needed to be left open to let the air in the box escape when creating a vacuum in the setup, otherwise the filters would have been destroyed because they provide the weakest part in the construction.

The diode used inside the box is the model AXUV100 produced by International Radiation Detectors Inc. and it provides us with a near theoretical quantum efficiency due to the absence of a surface dead region [3]. We placed the photodiode in front of the slit to be able to detect the whole energy and not only the part being not cut by the slit. Placing the diode behind the spectrometer instead would lead to lower intensities and easier detectability of a single harmonic, but would make the calculations harder and introduce more error sources. It is also extremely difficult to actually mount the diode behind the spectrometer and still be able to use the MCP, while mounting it in front of the slit with that condition can be done rather easily.

The diode is connected to an amplifier, a current-to-voltage converter of known resistance ($2.2\,\mathrm{k\Omega}$) and then to an oscilloscope. The oscilloscope, a Tektronix TDS 210, can be connected to a computer by using a GPIB-USB device from National Instruments.
A program written by Anders Persson called Tektrans allowed us to store both the picture on the oscilloscope screen and the raw data for further calculations. When having no gas pumped into the cell, we could not see any voltage and therefore deduced that our stray light protection and the filters were sufficient. The photodiode did however saturate at a voltage of about -2.9 V that was reached in a few cases. It is therefore recommended to use three filters (or thicker filters) when performing similar measurements next time.
Due to this saturation effect the highest energies we measured are actually slightly below the real values.

The oscilloscope was set to one vertical unit equaling 500 mV and one horizontal unit equaling 5 μs for every measurement.
A typical series of measurered voltages can be seen in Figure 6.4.

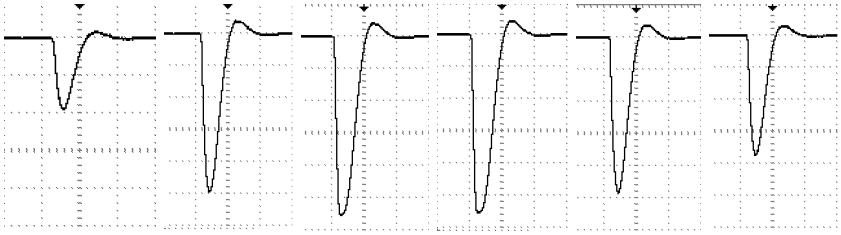

Figure 6.4: Different oscilloscope data for iris diameters (from left ro right) 11 mm, 12 mm, 14 mm, 16 mm, 17 mm and 18 mm and a 15 mm cell, one vertical unit representing 500 mV and one horizontal unit 5 μs using 1.2 bar pressure, 150 mJ input energy before compression and 40 fs pulses

A fast increase in the measured voltage can be observed, followed by a region with relatively small changes, before decreasing faster again.
The fast decrease may not be completely visible with just the pictures in Figure 6.4, but Figure 6.5 should show it quite clearly when comparing it to the previous pictures.

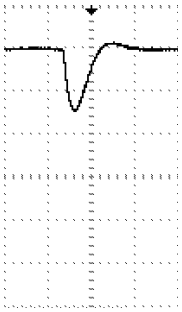

Figure 6.5: Oscilloscope screen for 27 mm iris diameter and a 15 mm cell using 1.2 bar pressure, 150 mJ input energy before compression and 40 fs pulses

After taking the data from the oscilloscope and storing it on the computer, we have to process it in a certain way to actually get the energy of the generated harmonics.
For this we need the frequency spectrum described in Section 5.4.
First a χ^2 calibration is done to find out whitch harmonic orders we are actually dealing with.
Therefore an order is assumed and the position of each harmonic (in pixels) is plotted over λ for the assumed wavelengths.

If the assumed order was correct, a linear function should fit through the points with extremely low error (hence a very small χ^2 value).
If the assumption was wrong, another order is assumed until the right order for the harmonics seen on the screen is found.

The harmonics observed by us are normally starting with the 15^{th} and range up to the 29^{th} order.

The grating in the spectrometer has a certain efficiency depending on the wavelength of the incoming light. This efficiency function is unknown to us but leads to the fact that we see less intense lower order harmonics in the spectrum (e.g. the 15^{th} order is normally seen way weaker than the 23^{rd} order).
To compensate this effect, we assume to work in the plateau region when dealing with the lower order harmonics we see.
We take an average of the intensities of the harmonics from 17^{th} to 21^{st} order and apply this average for the lower harmonics (down to the 11^{th}).

With this we can now get a relative intensity spectrum of all the harmonics we see.

The total number of electrons produced by the harmonic beam in the photodiode is now being calculated:

$$\int \frac{U}{RG} dt = \int I dt = C \tag{6.1}$$

$$\frac{C}{e} = N_e \tag{6.2}$$

With U being the voltage registered by the oscilloscope, R being the resistance, G the gain, I the current reaching the current-to-voltage converter, e the electron charge, C the charge registered by the oscilloscope and N_e the total number of produced electrons.

From this we can calculate the number of incoming photons, because we know the following equation:

$$N_e = \sum_k \alpha_k N_p \eta_k \tag{6.3}$$

Where k is the harmonic order, α_k the relative intensity of the k^{th} harmonic when hitting the photodiode (meaning that $\sum_k \alpha_k = 1$), η_k the quantum efficiency at the wavelength of the k^{th} harmonic and N_p the total number of photons hitting the diode.
The quantum efficiency is available at the homepage of the company that produced the photodiode and can be plotted as shown in Figure 6.6.

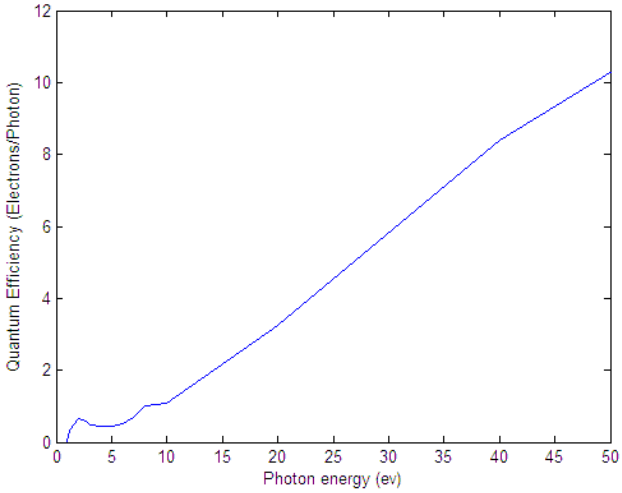

Figure 6.6: Quantum efficiency of the AXUV100 photodiode used in the experiments

To get the relative intensity of the harmonic when hitting the photodiode, we use the relative intensity calculated by using the spectrometer data and take the transmission function of our two 200 nm aluminum filters (seen in Figure 6.7) into account.

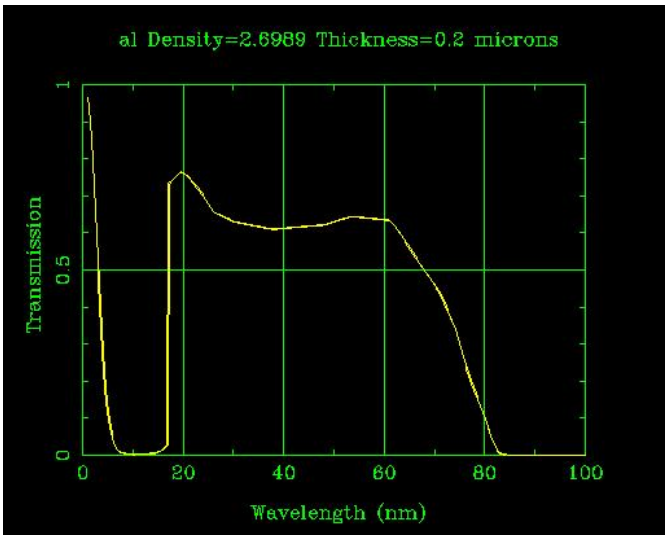

Figure 6.7: Transmission function of a 200 nm aluminum filter

With this we can calculate both the total number of photons hitting the diode N_p and the number of photons reaching the diode in each harmonic $n_k = \alpha_k N_p$.
Using the filter transimssion function again, we can easily calculate the number of photons in the harmonic beam before hitting the filter, the number of photons in each harmonic and, knowing that the energy of one photon of the k^{th} harmonic is $e_k = k \cdot e_g$, with e_g being the energy of one photon in the incident beam (800 nm wavelength $\rightarrow$ 1.55 eV), also the energy in each order, as well as the total energy for all our measured harmonics.

The total number of photons in the 11^{th} to 27^{th} harmonic is typically in the order of 10^{10}. The optimum energy was reached with a 19 mm gas cell and 20 mm iris diameter, all other parameters were unchanged (150 mJ input energy before compression, 1.2 bar pressure, 40 fs pulses). The total energy was 7×10^{-8} J, the total number of photons 1.66×10^{10}. The distribution was as following:

harmonic order	11	13	15	17	19	21	23	25	27
photons in 10^9	4.57	1.75	1.63	1.77	1.75	1.86	1.55	0.92	0.79
energy in 10^{-9} J	12.49	5.64	6.06	7.48	8.27	9.70	8.83	5.73	5.27

The energy of the incident pulse is around 18.2 mJ (around 97 % of 18.8 mJ measured for an iris diameter of 20 mm, because of the 3 % loss when passing the entrance window).
This gives us a conversion efficiency c of:

harmonic order	11	13	15	17	19	21	23	25	27
c in 10^{-7}	6.86	3.10	3.63	4.11	4.54	5.33	4.85	3.15	2.90

Adding up this numbers, we could convert $\approx 3.85 \times 10^{-6}$ of our input energy to harmonics in the order of from 11 to 27.

Due to all the assumptions that were mentioned earlier, this energies and photon numbers are significantly below the real value.
It can be estimated that the real energies (and therefore also conversion efficiencies) should be around a factor of 3 higher than what we calculated.

Putting all our observations into one graph (Figure 6.8), it can be concluded that the optimal iris diameter increases for longer cells and so does the total produceable energy. All graphs have in common that the energy increases very fast at small diameters before coming to its maximum. The following decrease is different for different cell lengths. The shorter cells (9 mm and 11 mm) start with a quite slow decrease in energy, while the longer cells (15 mm and 19 mm) show a somewhat faster decrease. The 19 mm cell seems to lack the region with relatively slow increases/decreases and shows a quite sharp peak at 20 mm iris diameter instead. All the other graphs show such a region (for example the 15 mm cell between 12 and 16 mm iris diameter).

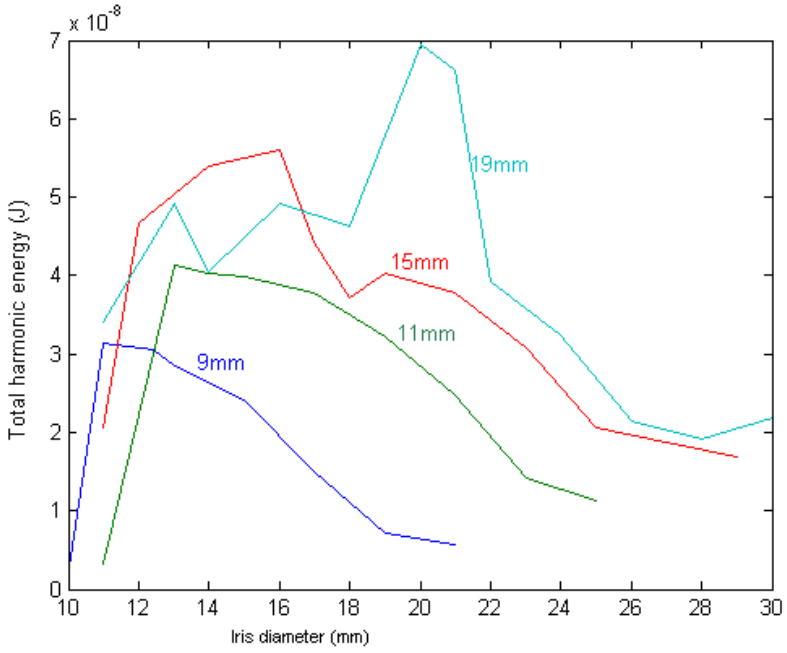

Figure 6.8: The total energies of the harmonics registered in dependence of the used iris diameters and cell lengths, using 150 mJ input energy before compression, 1.2 bar pressure and 40 fs pulses

This can be explained in the following way: After the needed energy to generate harmonics is reached with a certain iris diameter, further increasing of the opening leads to more energy being put into the incident beam, but also a smaller diameter of the beam in the focus and therefore a smaller interaction volume to actually generate harmonics.
In the region with only small changes in energy when varying the iris diameter, the decrease in interaction volume is somewhat compensated by the increase of input energy and the following increase in the non-linear interactions between gas and incident beam (optimizing the single-atom response).
After reaching a certain energy and a certain focal diameter (realized here by reaching a certain iris diameter), a further increase in intensity does not lead to more harmonic generation, but instead to way more ionisation in the medium. This, together with the further decrease in interaction volume, gives us the fast decrease in energy of the harmonics.

Chapter 7

Conclusion and Outlook

By inserting several new parts, from the $\lambda/2$-plate and the Brewster-window to the box for the photodiode, and changing existing ones, like the mount for the CCD-camera or the position of one of the turbopumps, a somewhat large step has been made to optimizing the HHG setup in Lund.

With these changes, more than one order of magnitude could be gained when comparing our energy measurements to the ones done about four years ago [5].

But most important: The alignment needed before doing any experiments with the HHG setup can now be done way faster compared to before and a shorter period of time is needed until a sufficient vacuum quality is reached. That, and hopefully also the procedures explained in this report, should help the groups working with this setup in the future to waste less time before being able to "do real physics".

More changes to the setup are already planned and will doubtlessly be made in the near future, the change to a lens with 4 m focal length and the building of a proper $\omega - 2\omega$ interferometer for use with that lens to just name two.

Those changes will hopefully (and most certainly) contribute further to optimizing the setup.

Bibliography

[1] L. Roos, Optimisation and Application of Intense High-Order Harmonic Pulses, Lund Reports on Atomic Physics, LRAP-276, Lund University, August 2001

[2] Tobias Eberle and Jan Klemmer, Design, Construction and Study of a new Gas Target for High-Order Harmonic Generation, Lund Reports on Atomic Physics, LRAP-371, Lund University, January 2007

[3] International Radiation Detectors Inc., www.ird-inc.com

[4] Per Johnsson, Attosecond Optical and Electronic Wave Packets, Lund Reports on Atomic Physics, LRAP-363, Lund University, 2006

[5] Allan Johansson, Application of Short Extreme Ultraviolet Pulses to the Spectroscopy of Atoms and Molecules, Lund Reports on Atomic Physics, LRAP-301, Lund University, May 2003